Acute anaphylactic and multiorgan inflammatory effects of Comirnaty in pigs: evidence of spike protein mRNA transfection and paralleling inflammatory cytokine upregulation

László Dézsi[1,2,**], Gábor Kökény[2,3**], Gábor Szénási[2,3], Csaba Révész[1,2,3], Tamás Mészáros[1,2,4,5], Bálint A. Barta[5], Réka Facsko[1,2,5], Anna Szilasi[6], Tamás Bakos[1], Gergely T. Kozma[1,4], Attila B. Dobos[5], Béla Merkely[5], Tamás Radovits[5], János Szebeni[1,2,4,7*]

[1] Nanomedicine Research and Education Center, Department of Translational Medicine, Semmelweis University, Budapest, Hungary
[2] Department of Translational Medicine, Semmelweis University, Budapest, Hungary
[3] International Nephrology Research and Training Center, Semmelweis University, Budapest, Hungary
[4] SeroScience Ltd., Budapest, Hungary
[5] Heart and Vascular Center, Faculty of Medicine, Semmelweis University, Budapest, Hungary
[6] Department of Pathology, University of Veterinary Medicine, Budapest, Hungary
[7] Translational Nanobioscience Research Center, Sungkyunkwan University, Suwon 16419, Korea

Abstract

Background and Purpose

Rare but serious adverse events (AEs) associated with mRNA-lipid nanoparticle (LNP) COVID-19 vaccines, such as Comirnaty and Spikevax, include acute and chronic inflammatory reactions, the mechanisms of which remain poorly understood. This study aimed to investigate these effects using a porcine model.

Experimental Approach

Naïve and anti-PEG antibody-sensitized pigs were intravenously injected with Comirnaty. Acute anaphylactic responses were assessed through hemodynamic monitoring, hematological changes, and plasma inflammatory markers. Multiorgan inflammatory effects were evaluated by qPCR detection of spike protein (SP) mRNA uptake and inflammatory cytokine gene expression in seven organs over 6 hours. Histopathology and immunohistochemistry were also performed.

Key Results

Severe cardiopulmonary distress developed within minutes of repeated i.v. injections of Comirnaty. qPCR revealed predominant SP mRNA accumulation in liver and PBMCs, with spleen, kidney, lymph nodes, heart, and brain also affected in 40–90% of animals. Repetitive PBMC transfection showed reversible mRNA peaks at 15 minutes, followed by rapid decay. Expression of proinflammatory cytokines (IL-1RA, CXCL10, TNF-α, CCL2) paralleled mRNA uptake, suggesting a causal relationship. Cytokine profiles varied by organ (e.g. IL-1RA in kidney, CCL2 in PBMCs). Histologic abnormalities and SP immunopositivity were noted in kidney, heart, and brain. Booster injections replicated PBMC transfection kinetics observed at first dose.

Conclusions and Implications

This porcine model reveals systemic anaphylactic reactivity and multiorgan SP mRNA transfection following i.v. injection of mRNA-LNPs, resulting in organ-specific inflammatory responses. These findings provide mechanistic insights into the rare vaccine-related AEs and may support future efforts to improve the safety of the mRNA-LNP platform technology.

Key words: circulation, COVID-19; inflammation, mRNA, LNP, PCR, spike protein, anaphylaxis, complement

*Corresponding author
**Shared first authors

1. Introduction

Adverse events associated with mRNA vaccines can be both acute and chronic. Among the acute reactions, anaphylaxis is the most serious, as it can be fatal in a small subset of susceptible individuals. Although exclusion of individuals with severe allergies from vaccination has helped reduce this risk, the overall incidence of anaphylaxis during the mass mRNA vaccination campaign was still reported to be 66-fold higher than that associated with all influenza vaccines. For this reason, clarifying the mechanism of vaccine-induced anaphylaxis remains to be a relevant study aim, pursued in the first part of our study.

However, anaphylaxis has been relegated to secondary concern compared to more frequent and less manageable chronic adverse events, which constitute key components of post-vaccination syndromes (PVS), and which are predominantly of inflammatory and/or autoimmune origin. Several hypotheses have been proposed to explain these effects, many of which emphasize the role of lipid nanoparticles (LNPs). These particles are used to deliver the mRNA encoding the spike protein (SP) to immune cells to initiate anti-SP immunogenicity. A central concern is the occurrence of multisystem inflammation resulting from pan-organ transfection with a toxin, driven by the systemic distribution of fusogenic LNPs.

The present study aimed to utilize pigs as a large animal model to investigate key mechanisms underlying both the acute anaphylactic and chronic inflammatory AEs of mRNA vaccines.

2. Results

2.1. The acute anaphylactic reactogenicity of Comirnaty

Pigs respond to i.v. administration of Comirnaty with transient hemodynamic, hematologic, and inflammatory mediator changes, most notably pulmonary hypertension, granulocytosis, and thromboxemia; a symptom triad characteristic of complement activation-related pseudoallergy (CARPA) (Dezsi et al., 2022). This reaction occurs in approximately 60% of pigs (6 out of 14), and in rare cases (1 out of 14), it progresses to anaphylactic shock. The hypersensitivity can be exacerbated by prior sensitization through immunization with PEGylated liposomes (Doxebo), after which all animals develop anaphylaxis to Comirnaty (Barta et al., 2024). Similar results were previously obtained with Doxebo injections (Kozma et al., 2019), and this analogy enabled the identification of both shared and distinct features of the two nanoparticles' reactogenicity.

2.2. Induction of anti-PEG hyperimmunity

The mean anti-PEG IgM level in the present study rose 200-fold over baseline a week after immunization with Doxebo, and reached a level roughly 20-fold higher than the anti-PEG IgG reached (SFig 1). Together with the similar earlier findings (Kozma et al., 2019), these results confirm the strong anti-PEG immunogenicity of Doxebo and reveal a striking preference of anti-PEG IgM binding vs. anti-PEG IgG in pig blood. Given the opposite pattern observed in humans, where PEG preferentially binds anti-PEG IgG (Kozma et al., 2019), and considering that normal serum IgG concentrations in pigs are approximately 10-fold higher than those of IgM (15–30 mg/mL vs. 1-3 mg/mL, respectively), this affinity of

PEG to anti-PEG IgM rather than IgG is counterintuitive and will be further explored in the Discussion.

2.3. Acute hemodynamic changes

Beyond reproducing the anaphylactic reactivity of Comirnaty as a test for the pigs' immune competency, the specific goal of repetitive injections of the vaccine at a high dose (5X human vaccine dose) was to compare the Comirnaty reactions to those caused by similar amounts of PEGylated liposomes, Doxebo, and thus gain further insight into its activation mechanism.

The first injection led within minutes to massive PAP, SAP and HR changes, some requiring CPR + epinephrine for survival (Figure 1). However, the patterns of simultaneously recorded PAP, SAP and HR curves were different after the repeated injections in all 6 additional reactions shown in SFigure 1. Notably, the pig in Panel A showed tachyphylaxis, while other pigs responded to consecutive injections with various hemodynamic changes. In essence, the time course and pattern of blood pressure changes caused by Doxil and Doxebo were remarkably similar, attesting to the same underlying mechanism of reactivity, namely C activation. On the other hand, while the hemodynamic effects of recurring injection of Doxil (Szebeni et al., 2012) and Doxebo (Kozma et al., 2019) were tachyphylactic, matched amounts of Comirnaty boluses lipid showed variable tachyphylaxis; full in some animals while absent in others. Panel D shows that the majority of pigs were low reponders to CMT treatments, and about half of them were tachyphylactic. These data align with the multicausal, mixed classical and alternative pathway activation of C

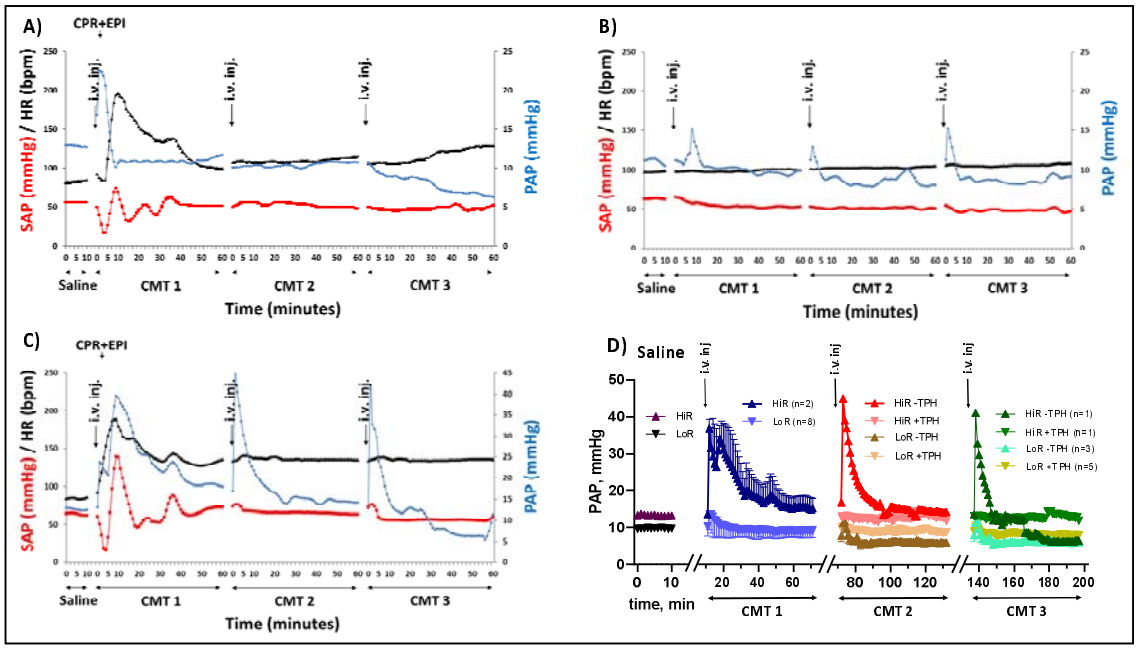

by Comirnaty (Bakos et al., 2024).

Figure 1. Acute hemodynamic changes after three consecutive injections of Comirnaty (CMT) applied in 5X human vaccine dose, roughly ~ 0.1 mg lipid/kg. A-C. Typical changes out of 10 similar experiments showing the individual variations. SAP, systemic arterial pressure, PAP, pulmonary arterial pressure, HR, heart rate. Three i.v. injections (i.v. inj.) of CMT are denoted by CMT 1 – CMT 2 – CMT 3; CPR+EPI – cardiopulmonary resuscitation with intracardiac administration of epinephrine. D. PAP changes are mean ± SEM and

categorized by the type of reactions. HiR – high responders, LoR – low responders; -TPH, without; and +TPH, with tachyphylaxis.

2.4. Acute cell and inflammatory marker changes in blood

Figure 2A shows that consecutive administrations of vaccine boluses led to 10-20% leukocytosis after each injection, without return to baseline after the individual injections. These additive rises were most likely due to bone marrow release of stored neutrophils and led to a lasting (> 6 h), up to 60% leukocytosis, implying active inflammatory, infectious, or immunological process (Christopher & Brounts, 2010; Ndeupen et al., 2021). The proinflammatory nature of mRNA-LNPs have been associated with a vicious cycle of cytokine release and C activation (Ndeupen et al., 2021; Nurnberger et al., 1994; Szebeni, 2025a,b) and the data presented next show parallel induction of these processes as well, thus proving that the leukocytosis is a consequence of the vaccine's proinflammatory effect.

Figure 2B shows the other characteristic blood cell effect of immune active nanoparticles: transient thrombocytopenia. This change was observed only after the first vaccine injection, and it could not be repeated with further injections. Such thrombocytopenia is a well-documented consequence of leukocyte and platelet activation, as well as pulmonary endothelial cell stimulation, mediated by the anaphylatoxins C3a and C5a. This process involves the formation of platelet–leukocyte aggregates and their transient adhesion to pulmonary endothelium, a phenomenon referred to as pulmonary marginalization. These interactions contribute to platelet sequestration and reversible thrombocytopenia during systemic inflammatory reactions (Guo & Ward, 2005; Sims & Wiedmer, 1991).

Consistent with the above-delineated role of C activation in leukocytosis and thrombocytopenia, we found laboratory evidence of C activation: sudden rise of C3a anaphylatoxin on the same time course where blood cell changes occur (Figure 2C). Similar changes were observed with TXB2, the stable metabolite of TXA2, the immediate effector of pulmonary and coronary vasoconstriction (Figure 2D). The reaction was partially tachyphylactic, just as the hemodynamic response, attesting to causal relationship between these processes (Bakos et al., 2024).

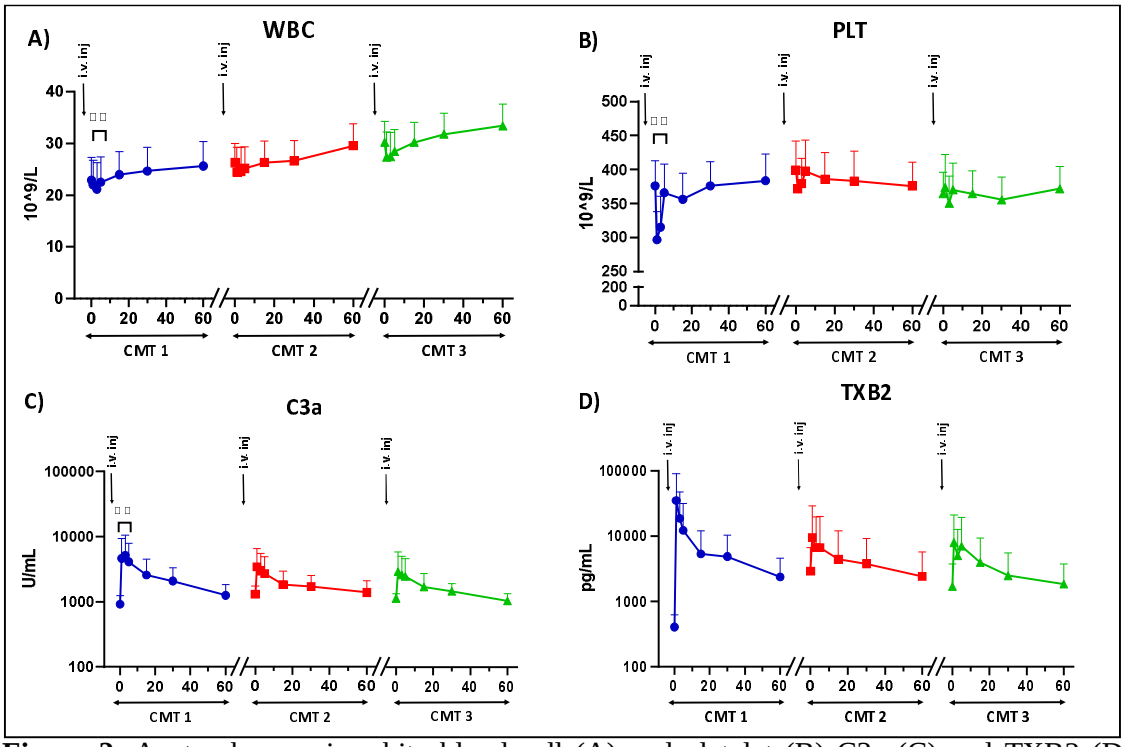

Figure 2. Acute changes in white blood cell (A) and platelet (B) C3a (C) and TXB2 (D) counts after three consecutive injections of Comirnaty in pigs. Mean ± SEM, n= 9 pigs

2.5. Pilot study findings on intramuscular vaccine-induced CARPA

In a preliminary investigation we assessed the potential for i.m. administered vaccine boluses to induce CARPA. The study involved two pigs: one developed tachycardia and fever, and the other, in which rebleeding was noted post-injection, exhibited signs of anaphylaxis. These outcomes support the notion that even i.m. vaccination may result in systemic exposure via vascular leakage or inadvertent intravascular entry (Dézsi et al, unpublished observations). Nonetheless, given the limited sample size, no conclusions can be drawn regarding the incidence or predictability of such reactions.

2.6. Uptake of SP mRNA by different organs

2.6.1. Peripheral blood mononuclear cells (PBMC)

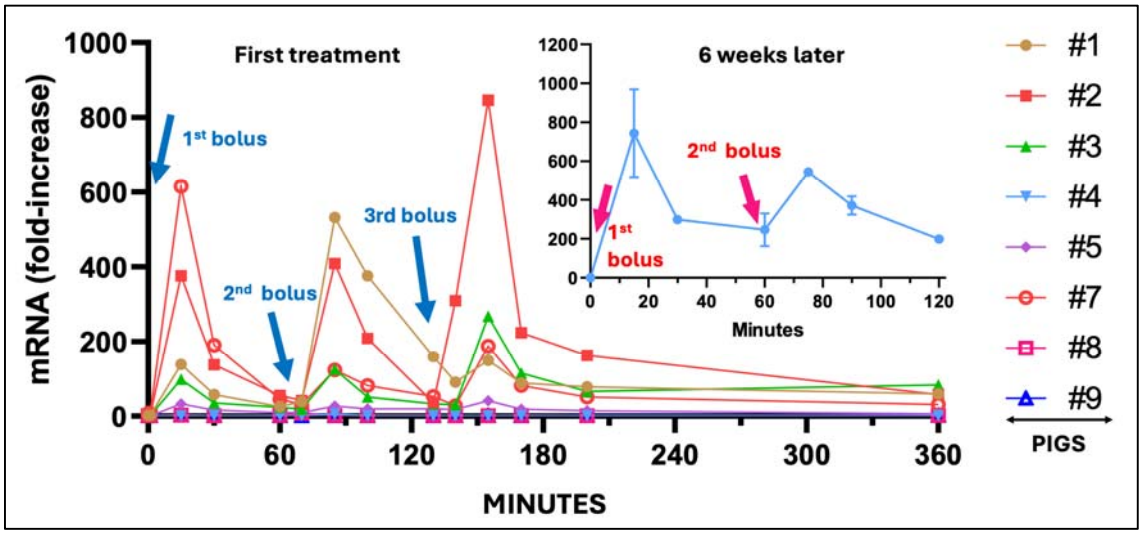

Figure 3. Kinetics of SP mRNA uptake by PBMCs of pigs following three consecutive bolus injections of Comirnaty (blue arrows). Fold increase means the mRNA level normalized to baseline in SPF animals. Curves with different symbols are individual data in 9 pigs, labeled with numbers (see key). The insert shows corresponding data six weeks after the initial Comirnaty treatment, simulating the effects of booster immunization. Here the injections are shown with red arrows.

As shown in Figure 3, three consecutive injections of Comirnaty led to variable SP mRNA accumulation in PBMCs across different pigs, peaking around 15 minutes and returning to near baseline within an hour. Maximum mRNA uptake, corresponding to 400–600-fold increases over baseline, was observed in two pigs out of 9 (#2 and #7), while the remaining animals showed either clearly detectable (#1 and #3) or minimal increases (#4, #5, #6, #8, and #9). Notably, uptake up to about 100-fold increase over baseline was observed with most animals even after 6 h.

The insert in Figure 3 further demonstrates that in the chronic study, a similar biphasic rise and fall of SP mRNA levels occurred following injection of the same vaccine doses six weeks after the initial treatment, which emulates booster vaccination. This indicates that neither the initial acute anaphylactic reaction and later, the gradually developing anti-SP and anti-PEG immune response interfered with the instant mRNA-LNP uptake of PBMC.

As for the human relevance of rapid mRNA-LNP uptake by pig blood cells after i.v. administration, several studies have demonstrated that a small fraction (~3%) of the mRNA-LNPs can enter the bloodstream shortly after i.m. injection (Pardi et al., 2015; Pfizer Australia, 2021). Thus, the above pig findings may apply to a small fraction of i.m. injected vaccine in humans and suggest that whatever amount of mRNA-LNP gets in blood, it can almost instantly transfect PBMCs, primarily monocytes, which can phagocytize the LNPs. The consequences of uptake and the swift intracellular degradation of the mRNA is addressed in the Discussion in detail.

2.6.2. Transfection of pig organs by mRNA-LNPs

Figure 4 shows that 6 h after vaccine injections, in addition to PBMC, 6 other organs of 9-11 pigs displayed varying increases of cellular levels of SP mRNA, indicating universal, although individually highly variable transfection of organ cells with SP mRNA. For example, the livers of all 11 pigs displayed SP mRNA accumulation, with variance over 3 orders of magnitude. The splenic uptake in 9/11 animals ranged between 10 and 3000-fold, while the corresponding lymph node and PBMC ratios were 10/11 and 7/11, respectively, up to about 100-fold increase. The kidney and heart uptake in 7/11 and 4/11 pigs ranged up to 10-fold, while near all, 9 of 11 pigs showed a minimal uptake of mRNA by the brain. These data provide evidence that the vaccine nanoparticles can transfect both the blood cells and different pig organs on a time scale of minutes to hours after entering in blood.

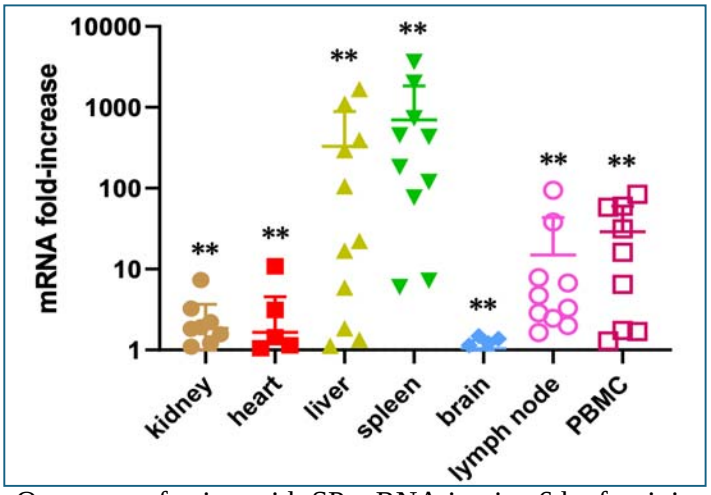

Figure 4. Organ transfection with SP mRNA in pigs 6 h after injection of Comirnaty. Values are >1 fold-increases (mean ± SD, n=9-11) from the PCR analysis relative to the SPF control. Values < 1 were considered 0 (baseline). Various symbols visualize differences in gene upregulation. Symbols for each gene identify different animals.

2.6.3. Histologic alterations in the different in pig organs

Figure 5. shows some notable histologic alterations in different pig organs at 6h. Detailed information on all histopathologic evaluations is provided in STable 2. We found no significant pathological changes in sections of skin, lymph node, myocardium, and spleen tissues 6 hours after vaccination. However, we could observe neuropil vacuolization in almost all brain samples and vascular edema in some cases. Livers of pig #1 and #9 showed mild sinusoidal hyperemia, and in the case of pig #3, we detected multifocal necrosis and moderate periportal hepatitis. Kidneys of #4, #5, and #9 showed multifocal tubular dilation. Tubular epithelial cells were either flattened or cuboidal.

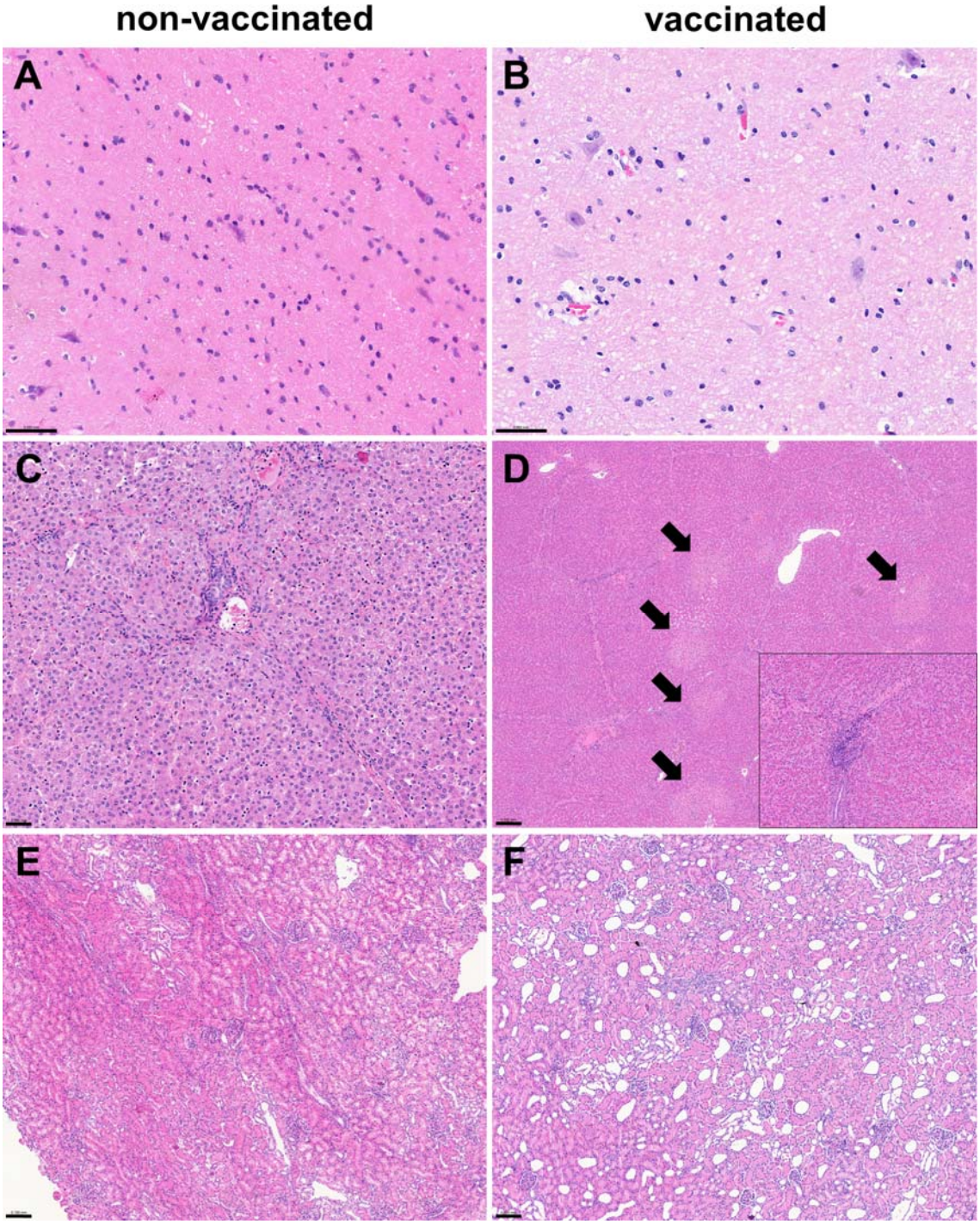

Figure 5. Comparison panel of SPF control tissues (A, C, E) and specimens of vaccinated pigs containing pathologic lesions (B, D, F). A: brain tissue with normal histologic structure; B: brain tissue showing mild vacuolization of neuropils, and vascular edema (bar=50 µm). C: normal architecture of liver; D: multifocal necrosis in the liver parenchyma (arrows). The inset shows the moderate mononuclear cell infiltrate at the portal/periportal area (bar=500 µm, inset: bar=100 µm). E: renal tissue with physiologic histologic structure; F: multifocally and mildly dilated tubules in the cortex of the kidney (bar=200 µm). All sections are stained with H&E.

2.7. Upregulation of proinflammatory cytokine genes in PBMC 6 h after injection of Comirnaty

The transient accumulation and decomposition cycles of SP mRNA in PBMC (Figure 3) was associated with variable upregulation of IL1-RA, CXCL10, TNF-α and CCL2 genes at 6 h post-injection (Figure 6). Interestingly, CCL2 gene upregulation in the 5-60-fold range was significantly more expressed than the maximal 10-fold increases observed in for the other 3 cytokines' mRNA, although IL-1RA was particularly expressed in the PBMC of 2 of 11 pigs. As discussed earlier at Figure 4, these cytokine releases can most easily be explained by monocyte activation, whereupon the release of IL-1β, IL-6, CCL3, CCL4 were reported before (Zelkoski et al., 2025).

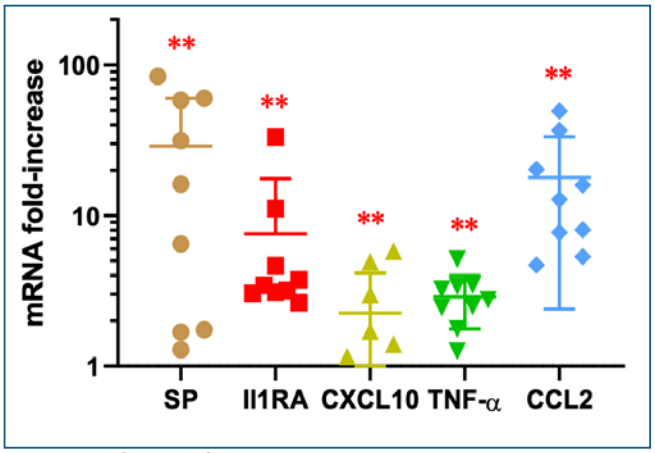

Figure 6. Upregulation of proinflammatory cytokine genes in PBMC 6 h after injection of Comirnaty (mean ± SD, n=9). Various symbols visualize differences in gene upregulation. Symbols for each gene identify different animals.

2.8. Upregulation of proinflammatory cytokines in pig organs 6 h after injection of Comirnaty

Similarly to PBMC, the vaccine-induced SP mRNA was associated with variable upregulation of different proinflammatory genes in different pig organs at 6 h after injection of Comirnaty. As shown if Figure 7, the liver accumulated the most SP mRNA, which was followed by up to 100-fold accumulation of IL1-RA, and up to 10-fold CXCL10, TNF-α and CCL2 genes at 6 h post-injection

Overall, these data prove the utility of the model for quantitative assessment of the organ distribution of intact SP mRNA after vaccination.

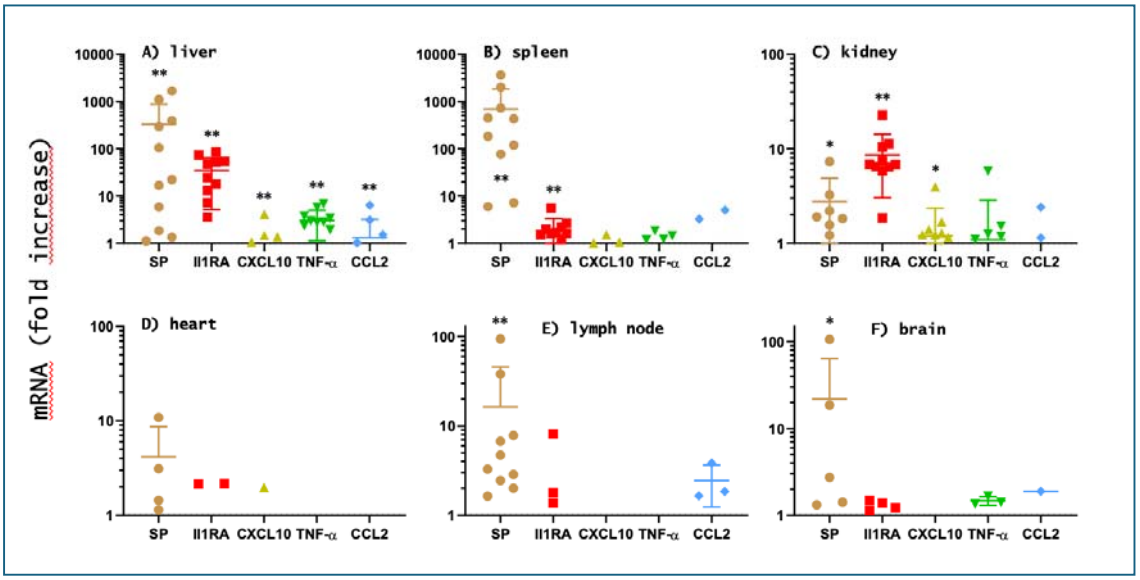

Figure 7. Association of SP mRNA transfection with proinflammatory cytokine gene upregulation in different pig organs 6 h after Comirnaty injection (mean ± SD, n=9-11). Various symbols visualize differences in gene upregulation. Symbols for each gene identify different animals.

2.9. Immunostaining of pig organs for SP expression

Immunostaining for SP in kidney and heart tissues revealed a strong positive reaction in renal tubules (Figure 8A) and a milder positivity in the myocardium (Figure 8B) of vaccinated pigs (right panel), as compared to the tissues of non-vaccinated control (left panel). SP protein was also expressed in brain cells (Figure 8C, see arrows) of vaccinated pigs 6 h after the injection of Comirnaty (lower panel), but was not detected in non-vaccinated pig brain tissue.

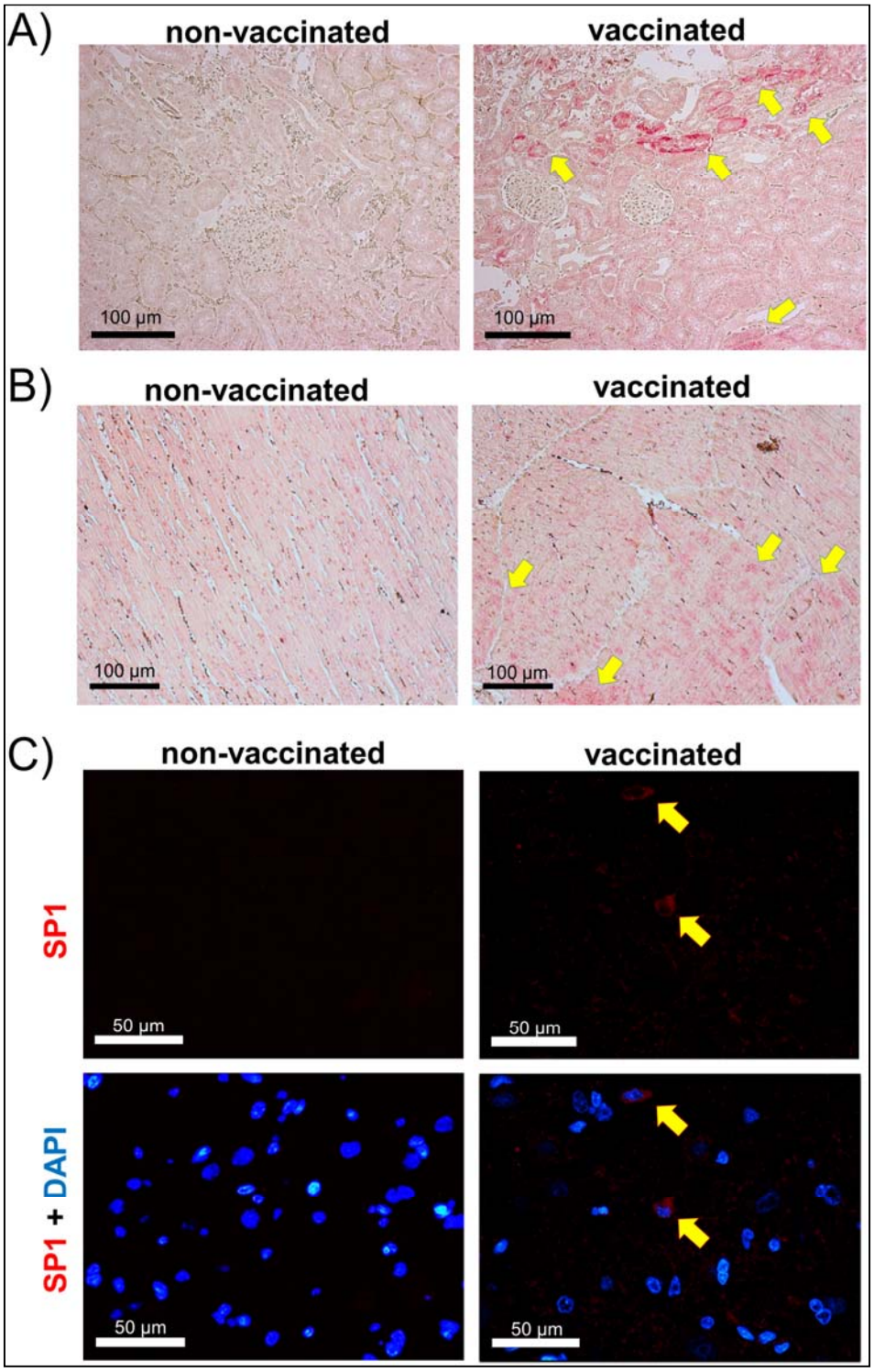

Figure 8. Immunohistochemistry for SP protein expression in pig kidney (A), heart (B) and brain (C) 6 h after injection of Comirnaty or vehicle. Arrows point on the SP1-positive stain of kidney tubules (A) and myocardial tissue (B) as well as SP1-positive brain cells (C). Scale bar=100µm (A, B) and 50µm (C). DAPI (blue) stains the nuclei in immunofluorescent slides.

3. Discussion

3.1. The challenge of vaccine-induced AEs

Since the introduction of DNA- and mRNA-based COVID-19 vaccines designed to encode antigens instead of delivering them directly, concerns are growing about the evidence of a relatively broad spectrum and a high incidence of severe AEs caused by these "genetic" vaccines. The phenomenon has led to the distinction of a novel diagnostic category: "post-vaccination syndrome" (PVS) (Bhattacharjee et al., 2025; Krumholz et al., 2023; Oueijan, Hill, Ahiawodzi, Fasinu, & Thompson, 2022; Palmer et al., 2023; Shrestha & Venkataraman, 2024), whose chronic, occasionally disabling complications can be considered as a iatrogenic orphan disease" (Janos Szebeni, 2025). While the absolute incidence of AEs is low (0.03–0.5%), the global administration of more than 5.3 billion doses implies that the number of PVS cases is non-negligible, warranting further scrutiny of both the vaccines and the underlying technology. The gravity of the problem controversy is reflected by the facts that several countries have suspended, restricted, or issued contraindications for mRNA COVID-19 vaccines. In the US, legislative efforts to restrict or ban mRNA vaccines have been introduced in several states, and as of May 2025, the Centers for Disease Control and Prevention (CDC) has updated its mRNA vaccine recommendations to focus primarily on individuals at higher risk of severe illness. Feeding the public confusion, the scientific community remains divided over the technology, with both critical and supportive perspectives expressed with strong conviction. Given this polarization, it is essential to continue investigating these issues with scientific rigor to better elucidate the mechanisms underlying the reported AEs.

3.2. Specific study goals

Previous reviews have provided both AE-focused and broader analyses of the potential causes of AEs, including focus on anaphylaxis and multiorgan inflammation (Lamprinou, Sachinidis, Stamoula, Vavilis, & Papazisis, 2023; Szebeni, 2025a,b). The present experimental study builds upon this foundation, offering further evidence that supports two key concepts: (i) the CARPA and anti-PEG antibody theory of anaphylaxis, and (ii) the whole-body distribution of inflammatory mRNA-LNPs as a mechanism underlying systemic, multiorgan inflammation. The sections below explore these findings in detail.

3.3. Vaccine-induced anaphylaxis and its modeling

Anaphylaxis is the most life-threatening acute AE associated with mRNA COVID-19 vaccines. Although its overall incidence is low (in the 0.001-0.04% range (Anis et al., 2022; Blumenthal et al., 2021; Shimabukuro, Cole, & Su, 2021; Janos Szebeni, 2025; Warren et al., 2021), it is still significantly higher compared to that of conventional vaccines, such as flu (Janos Szebeni, 2025). Of particular relevance to our study, Shavit et al. (Shavit et al., 2021) demonstrated that in individuals with a history of severe allergies, the incidence of Comirnaty-induced anaphylaxis was 0.7%, i.e., at least 20 times higher than that observed in the general population (Shavit et al., 2021). This shows that special sensitivity for these reactions exists, giving rationale to use naturally hypersensitive animal models to study the phenomenon, such as the porcine CARPA model (Dezsi et al., 2022; Barta et al., 2024; Szebeni, 2024), and its PEGylated liposome (Doxebo)-sensitized version wherein the animals are made hyperimmune against PEG (Barta et al., 2024).

3.4. The hyperimmune pig model and its human relevance

In the hyperimmune pig model all (n=9) pigs developed anaphylactic shock from i.v. injection of 1/3 human dose of Comirnaty (0.01 mg lipid/kg) (Barta et al., 2024), which is the same dose that caused anaphylaxis in 0.7% of highly allergic people (Shavit et al., 2021). (The reference to lipid content is due to the fact that the anaphylaxis is primarily caused by the lipids in the vaccine (Janos Szebeni, 2024)). Thus, this pig experiment provides a model for the 0.7% of allergic people who developed anaphylaxis to Comirnaty (Shavit et al., 2021). The incidence of severe allergy (e.g., anaphylaxis to food, drugs, insect stings) is 1-3% of the population (Lieberman, 2008; Turner et al., 2017), and 0.7% of 1-3% is 0.007-0.021%, higher than the lower threshold of the mentioned range of vaccine-induced anaphylaxis in the whole population (>0.001%) (Anis et al., 2022; Blumenthal et al., 2021; Shimabukuro et al., 2021; Szebeni, 2025; Warren et al., 2021). This allows proposing that if the sensitivity of the pig model was the same as that of a normal, non-allergic human, ~4,800 pigs would show 1 anaphylaxis from the mRNA vaccine, and ~40,000 pigs 9 anaphylaxis in a row. Thus, the anti-PEG hyperimmune pig model may uniquely facilitate the in vivo study of vaccine-induced, and all other nanoparticle-induced anaphylaxis.

3.5. The deltoid leakage hypothesis in vaccine delivery

The pilot experiment described in the results section showed that the vaccine can gain rapid access to the bloodstream, which is in keeping with other studies reporting rapid intravasation of LNPs via lymphatic drainage, capillary absorption or accidental i.v. injection (Brogna et al., 2023; Kent et al., 2024). Thus, unlike traditional vaccines that are known to retain the antigen in tissue depots, the i.m.-administered mRNA-LNPs may occasionally distribute systemically via the bloodstream. This fact has been receiving little attention in the context of mRNA-LNP vaccines although the entry of i.m. injected LNPs into the bloodstream within hours had been described before the use of LNP for vaccination (Pardi et al., 2015), and a preclinical rat study on Comirnaty pharmacokinetics also showed leakage from the injection site and widespread distribution of labeled LNPs throughout the body, within hours, starting within minutes (Ltd, 2021). The experiment showed ~3% of injected LNP lipid in blood within 15 min after i.m. injection, and that its' plasma level doubled within 2-6 h (Ltd, 2021). In a quantitative study, Kent et al., showed that 4 h after the injection of Comirnaty in humans the vaccine lipid detected in plasma was in the 0.13-2.08 ng/mL range (Kent et al., 2024). Considering 38.5 mL plasma/kg in man (and pigs), the observed 100 ng lipid/kg effective anaphylactic dose in severely allergic people (Shavit et al., 2021) and in our hyperimmune pig model (Barta et al., 2024) translates to 2.6 ng vaccine lipid/mL. These values are close, but cause-effect relationship cannot be established as C activation is a rate-limiting step in vaccine lipid-induced anaphylaxis, and its lipid-dose dependence may be highly variable. Further studies in this direction might lead to an onsite test predicting the individual risk of anaphylaxis based on in vitro C assays.

3.6. The relevance of tachyphylaxis

A further clinically relevant observation in the present pig studies is that that three consecutive injections of 5X human vaccine (0.15 mg/kg lipid in each) dose induced similar, even more variable anaphylaxis as the low (1/3 human dose, 0.01 mg/kg) dose, suggesting no further acceleration of anaphylactic shock compared to that seen with the low, 0.01 mg lipid/kg low bolus dose. Also, the finding that repetitive administration of Doxebo in the hyperimmune model led to near full tachyphylactic reacions implying tolerance induction, while the vaccine-induced anaphylactic reactions to the same dose (1/3 HD) showed repeat reactions, with substantial interindividual variation, is consistent with stronger C activation by Comirnaty than Doxebo (Bakos et al., 2024).

3.7. Anti-PEG immunogenicity: the paradox of subclass reversal

We found up to 100-fold difference between the Doxebo-induced maximal rise of anti-PEG IgM versus IgG titers (Fig 1), which is consistent with or previous results, but goes against the human experience, showing an equal difference with IgG overweight. Given that normal serum concentrations of IgG and IgM in pigs are approximately 15–30 mg/mL and 1–3 mg/mL, respectively, antibody binding to PEG-coated plates is not proportional to the bulk levels of these subclasses in pig blood. This suggests that the plate-bound PEG discriminates between IgG and IgM in the case of the pig assay, possibly due to a specific biological or technical property, such as differences in antibody glycosylation, isotype structure, or affinity for PEG. Further investigation is warranted to clarify whether this represents a true immunological difference or a technical peculiarity of the porcine anti-PEG ELISA

3.8. The uptake of mRNA-LNP by PBMC

The effects of mRNA–LNPs on blood cells has received limited attention in the context of vaccine-induced systemic inflammation, which is a notable gap given the innate immune activity of granulocytes and monocytes. Our experiments showing almost immediate, non-tachyphylactic uptake of mRNA-LNPs on a time scale of minutes may represent a novel information, as previous analysis followed such uptake over days.

The identity of WBC subtypes responsible for vaccine uptake remains unclear. Since granulocytes, red blood cells and platelets are effectively removed from the PBMC upon ficoll preparation, the mRNA internalization that we see in Figure 5 most likely represents the combined uptake or adherence of nanoparticles by the T cells (~60–80%), B cells (~5–15%), NK cells (~5–15%), and monocytes (~10–20%). However, among these cells, endocytic and phagocytic uptake of mRNA-LNPs have only been demonstrated for monocytes (Ndeupen et al., 2021; Pardi, Hogan, Porter, & Weissman, 2018); T and B lymphocytes are thought to be generally involved in later events of specific immunogenicity (Ndeupen et al., 2021; Wei, Dong, Zhu, & Wang, 2024).

Monocyte uptake of mRNA-LNPs is in keeping with the fact that mRNA-LNPs can activate these cells through Toll-like receptor 4 (TLR4) and MyD88-dependent signaling, along with NLRP3 inflammasome activation, leading to the release of proinflammatory cytokines and chemokines into blood (Ndeupen et al., 2021; Pardi et al., 2018; Wei et al., 2024); T and B lymphocytes are generally involved in later events of specific immunogenicity (Ndeupen et al., 2021; Wei et al., 2024). These processes are associated by lysosomal disruption and the release of cathepsins into the monocyte cytosol, leading to apoptosis or necroptosis (Zelkoski et al., 2025). The upregulation of IL-1β, IL-6, and CCL3 genes in PBMC (Fig 7), provide further evidence for the implication of monocytes in vaccine-induced systemic inflammation. These data provide a mechanistic explanation for the observed proinflammatory cytokine release and monocyte toxicity in human PVS (Bhattacharjee et al., 2025).

As for the swift intracellular degradation of the mRNA, it is unexpected in light of several stabilizing modifications of the mRNA including the replacement of uridine with pseudouridine (Ψ) or N1-methylpseudouridine (m1Ψ) (Kariko, Buckstein, Ni, & Weissman, 2005), 5′ cap modification (Kauffman et al., 2016), optimization of the untranslated regions (UTRs) (Pardi et al., 2018) and Poly(A) tail engineering (Schlake, Thess, Fotin-Mleczek, & Kallen, 2012). The implications of these observations need to be explored in the future.

3.9. The clinical relevance and mechanism of multiorgan mRNA uptake

We report in the present study highly variable, but in some animal robust uptake of functional SP mRNA in all 5 studied organs (liver, spleen, heart, lymph node, kidney), except the brain. As expected from the mRNA-LNP tissue distribution, the liver, spleen and lymph nodes showed the most uptake in the overwhelming number of pigs, as well as the PBMC, which too contains LNP target cells (monocytes). What was a less predictable result is that the heart and the kidney of a portion of animals also took up the mRNA, which are not target tissues for the vaccine, yet display AEs, particularly the heart.

The mRNA uptake implies transfection of functional mRNA, a well-known feature of mRNA-LNPs, actually, this led to their clinical development as nucleic acid delivery agents (Cheng et al., 2023; Cullis & Felgner, 2024; Francia, Schiffelers, Cullis, & Witzigmann, 2020). One critical question is, however, what is the relevance of our and others' findings on transfection in the AEs of COVID-19 vaccinations, since all in vitro and in vivo experiment on this phenomenon had different conditions relative to real-life vaccination.

Taken together, our finding of substantial mRNA uptake and even SP expression after 6 h in the kidney align well with these assumptions and calculations. However, given the anatomical and physiological variability of organ circulation, it is perhaps not surprising that the mRNA uptake had substantial individual variation even in pigs, not to mention the immense human variation.

Regarding the mechanism of mRNA-LNP uptake by endothelial and other cells, it can be through endocytosis, either clathrin-, or caveolae-mediated, micropinocytosis, more in inflammatory or activated endothelium, and/or fusion, a distinguishing feature of ionizable lipid-containing LNPs (Cheng et al., 2023; Cullis & Felgner, 2024; Francia et al., 2020). It is very likely that this uptake process is rate limiting to transfection and determines the presence or absence of AEs of the target organ. Accordingly, the study of the cellular uptake of mRNA-LNPs may provide a predictor for inflammatory and autoimmune complications.

3.10. Inflammatory cytokines studied

The cytokines investigated in this study are critically involved in mediating inflammation and immune cell recruitment during immune responses and pathological conditions (Jaffer, Wade, & Gourlay, 2010; Kany, Vollrath, & Relja, 2019). Among them, IL-1 receptor antagonist (IL-1RA), CXCL10, tumor necrosis factor-alpha (TNF-α), and CCL2 play distinct yet interconnected roles. IL-1RA is an anti-inflammatory cytokine that inhibits IL-1 signaling, often upregulated as a compensatory response during inflammation. CXCL10 is a chemokine that recruits Th1 cells and NK cells, commonly elevated in viral and autoimmune conditions. TNF-α is a central proinflammatory cytokine that promotes cell recruitment, apoptosis, and systemic inflammation. CCL2 attracts monocytes and contributes to chronic inflammation and tissue damage. Together, these mediators reflect and drive inflammatory responses across diverse pathological settings (Jaffer et al., 2010; Kany et al., 2019).

3.11. Association of multiorgan mRNA uptake and inflammatory cytokine upregulation

Multisystem inflammatory adverse events, while rare, represent significant complications in a small subset of mRNA vaccine recipients. These events are characterized by inflammation across multiple organ systems and may resemble autoimmune or hyperinflammatory syndromes. Reported manifestations include myocarditis and pericarditis, vasculitis, autoimmune-like syndromes (e.g., lupus-like conditions, rheumatoid arthritis flare-ups), and neurological inflammatory disorders such as Guillain-Barré syndrome and

encephalitis. The underlying mechanism is hypothesized to involve innate immune activation triggered by the LNPs and SP expression in unintended tissues. However, the causal relationship between these elements remains unclear. Specifically, it is not yet established whether the SP and LNPs are coincidental processes independently inducing inflammation, or they act jointly in an additive or synergistic manner.

Our observations added further complexity to this puzzle inasmuch as they revealed a temporal, but not quantitative association between mRNA uptake and the upregulation of inflammatory cytokines across different tissues. Also, we found evidence for SP protein surfacing in the kidney and heart 6h after vaccination, which provides evidence for rapid translation of the mRNA to protein, hence ambiguity regarding individual roles of the mRNA and the SP in the ternary (LNP, mRNA, SP) cooperation in causing inflammation. Yet another complexity; the relatively high reproducibility of cytokine transcription profile among the animals was contrasted by substantial variation among the tissues, adding tissue-specificity to the inflammatory response. Taken together, establishing a consistent association between vaccine effects and inflammation represents an important step toward clarifying the mechanisms underlying inflammatory AEs, although the precise molecular interactions and downstream pathways within the vaccine-hit non-target cells remain to be elucidated.

3.12. Special focus on the heart

The heart has received particular attention regarding mRNA vaccine-associated AEs, as myocarditis and pericarditis have been among the most closely investigated safety concerns since the rollout of these vaccines (Bozkurt, Kamat, & Hotez, 2021; McCullough & Hulscher, 2025; Sindet-Pedersen et al., 2023). These conditions are often attributed to subclinical myopericarditis, an inflammation of the heart muscle and pericardial tissue. While most reported cases are mild and self-limiting, persistent abnormalities with reduced cardiac function have also been documented.

Notably, Boros et al. demonstrated the persistence of biochemically modified mRNA and its frameshifted protein products in inflamed and fibrotic cardiac tissues up to one month post-injection (Boros et al., 2024). In vitro, using isolated ventricular cardiomyocytes Schreckenberg et al. showed mRNA vaccine-induced production of the SP, leading to completely irregular contractions (Schreckenberg et al., 2024). This abnormality, linked to dysfunction of the cardiac ryanodine receptor (RyR2) and/or increased protein kinase A (PKA), recapitulate the severe, sometimes fatal arrhythmias reported particularly in young males during physical exercise (McCullough & Hulscher, 2025).

Our own data indicate that direct cardiac transfection and inflammation can occur as early as six hours after vaccine administration, suggesting that pathological changes may begin shortly after vaccination, even though the AEs emerge only weeks later, or after booster doses. The clinical importance of these findings lies in the potential for early identification of individuals at risk for cardiac complications, especially those with a history of heart disease, thereby enabling preventive interventions that may be lifesaving.

4. Outlook

The public and scientific communities remain polarized regarding the use of mRNA-LNP technology in vaccination, with both critical and supportive opinions often held with strong conviction. In such a climate, only rigorous scientific inquiry can advance understanding and establish evidence-based conclusions; a process that is increasingly gaining momentum.

Our study, conducted in a porcine model, aimed to contribute to this effort by providing new insights into the mechanisms of vaccine-induced anaphylaxis and the temporal dynamics

of mRNA transfection across various tissues. A deeper understanding of these phenomena may ultimately help improve the safety profile of the mRNA–LNP platform. It is essential to emphasize that this scientific investigation does not challenge the overall benefits of vaccination, nor does it take a position in the “pro- vs anti-vaccine” debate. Its sole purpose is to support the full realization of the potential of mRNA–LNP technology through critical, evidence-based research.

5. Methods

5.1. Pig studies

Landrace pigs were obtained from the Research Institute for Animal Breeding, Nutrition and Meat Science of the Hungarian University of Agriculture and Life Sciences (Herceghalom, Hungary). The SPF DanBred pigs were from Sano-Pikk Ltd., (Zsámbék, Hungary). The study involved 11 (+2 SPF) female and castrated male pigs in the 22–32 kg size range. They underwent a 1-week acclimation period in the experimental large animal housing facility before starting the experiments. Pigs were given standard laboratory pig diet and water *ad libitum*. All procedures were performed in accordance with ARRIVE guidelines and the guidelines of the Council Directive of the European Communities (86/609/EEC) and approved by the Pest County Government Office, under permission number: PE/EA/843-7/2020.

5.2. Immunization against liposomal PEG

In the first stage, animals were immunized against liposomal PEG by injecting them with liposomal doxorubicin (Doxebo). The preparation and characteristics of Doxebo were described earlier in detail (Kozma et al., 2019). In brief, the freeze-dried lipid components of Doxil were hydrated in 10 mL sterile pyrogen-free normal saline by vortexing for 2−3 min at 70°C to form multilamellar vesicles (MLVs). The MLVs were downsized through 0.4 and 0.1 µm polycarbonate filters in two steps, 10 times through each, using a 10 mL extruder barrel from Northern Lipids (Vancouver, British Columbia, Canada) at 62 °C. Liposomes were suspended in 0.15 M NaCl/10 mM histidine buffer (pH 6.5). The size distribution (Z-average: 81.17 nm) and phospholipid concentration of Doxebo (12.6 mg/mL) were determined as described earlier (Kozma et al., 2019). After taking pre-immune blood samples, the ani-PEG immunization was done by infusing 0.1 mg PL/kg Doxebo via the ear vein (suspended in 20 mL of saline) at a speed of 1 mL/min. The animals were then placed back into their cages until the 2nd blood sampling 7-10 days later, to screen for anti-PEG Ab induction. From that time, the animals showing seroconversion were subjected to the "CARPA induction" protocol with Comirnaty. One control animal was sham-immunized with PBS but was handled identically to the Doxebo-immunized pigs.

5.3. Treatment of pigs with Comirnaty i.v.

We report in this study data from 3 types of pig experiments. In one, pigs were treated with three consecutive i.v. injections of Comirnaty vaccine, where each treatment was followed for 1 hrs. Each Comirnaty injection contained cca. 6 µg mRNA/kg (150 µg mRNA/dose; 5X human dose). Thereafter, the animals were subjected to the “standard” CARPA protocol (Szebeni, 2024) as follows. After sedation in the porcine confinement area with an i.m. injection of 15 mg/kg ketamine (Gedeon Richter Plc. Budapest, Hungary) and 2 mg/kg xylazin (Produlab Pharma, Raamsdonksveer, Netherlands), the animals were carefully transported into the laboratory. Airways were secured by inserting an endotracheal tube. Anesthesia was induced with 2 − 2.5% isoflurane (Rompharm, Otopeni, Romania) in O_2. Unless otherwise specified, animals were allowed to breath spontaneously during the

experiments. Controlled ventilation was applied when continuous measurement of hemodynamic parameters necessitated invasive surgical interventions. Surgery was done after povidone iodine (10%) disinfection of the skin. To measure the pulmonary arterial pressure (PAP), a Swan-Ganz catheter (Arrow AI-07124, 5 Fr. 110 cm, Teleflex, Morrisville, NC, USA) was introduced into the pulmonary artery via the right internal jugular vein. A 15 G catheter was placed into the left femoral artery to record the systemic arterial pressure (SAP). Additional catheters were introduced into the left external jugular vein for drug administration, into the left femoral vein for venous blood sampling. Hemodynamic data were collected using instruments from Pulsion Medical Systems, and Powerlab, AD-Instruments (Castle Hill, Australia). In the above "acute" protocol, applied for 10 pigs, the animals were monitored for hemodynamic, blood cell and inflammatory mediator changes for 6 h before sacrificing them for organ collection. Blood was collected before and at 1, 3, 5, 15, 30 and 60 min after each Comirnaty injection.

In two cases of the acute studies, the animals obtained the same dose of the vaccine i.m., three times repeatedly (timed as above). The third type of study (5 pigs) was 'chronic", i.e. animals had previously been treated 2-times with i.v. Comirnaty vaccine 6 weeks before, applying the same doses as in the acute experiments. Blood withdrawals in these pigs were performed at 3 weeks and at 6 weeks, before and during the final "standard" CARPA experiment and organ collection. In six cases, a "booster" immunization (Doxebo) was applied one week prior to the study.

5.4. Blood Assays

Ten mL of venous blood was drawn from the pigs at different times into EDTA containing vacuum blood collection tubes (K3EDTA Vacuette, Greiner Bio-One Hungary, Mosonmagyaróvár, Hungary). 0.5 mL of blood was aliquoted for use in an ABACUS Junior Vet hematology analyzer (Diatron, Budapest, Hungary) to measure the following parameters of blood cells: white blood cell (WBC), granulocyte (GR) and lymphocyte (LY), platelet (PLT), red blood cell (RBC) count and hemoglobin (Hgb) concentration. For measuring thromboxane B2 (TXB2), a stable metabolite of thromboxane A2 (TXA2), 4 μg indomethacin (diluted in 2 μL of 96% ethanol) was mixed with 2 mL of anticoagulated blood to prevent TXA2 release from WBC before centrifugation at 2000× *g*, for 4 min at 4 °C. Another 2 mL of anticoagulated blood was directly centrifuged using the same settings to separate the plasma.

After centrifugation, the plasma samples were aliquoted, frozen, and stored at −70 °C until the TXB2 assay was performed as described in the kits' instructions. We used a commercially available ELISA kit (Cayman Chemicals, Ann Arbor, MI, USA) and an FLUOstar Omega microplate reader (BMG Labtech, Ortenberg, Germany).

5.5. Isolation of PBMC

The blood samples collected as described above were aliquoted, and one portion was used for peripheral blood mononuclear cell (PBMC) separation within 30 min after blood withdrawal. Briefly, 2 mL blood was transferred into a 15 mL tube and diluted with 2 mL phosphate-buffer saline (PBS pH 7.4). In a new 15 mL tube, 3 mL Ficoll-Paque media (GE Healthcare, Chicago, IL, USA) was pipetted into the bottom and the diluted 4 mL blood sample was carefully layered on top, centrifuged for 30 min at 400× *g*. The upper plasma layer was removed, and the leukocyte layer was transferred into a new tube containing 6 mL PBS, washed and centrifuged.

5.6. Quantitative RT-PCR in PBMC and different pig organs

The PBMCs were resuspended in 1 mL TriZol (Thermo Fisher Scientific, Waltham, MA, USA) and total RNA was extracted according to manufacturer's instructions. RNA pellet was resuspended in RNAse-free water and the RNA concentration was determined photometrically on a NanoDrop microphotometer (Thermo Fisher). One microgram of RNA of each sample was reverse-transcribed with the high-capacity cDNA reverse transcription kit from Applied Biosystems (Applied Biosystems/Life Technologies, Carlsbad, CA, USA) using random primers in a final volume of 20 μL. Quantitative real-time PCR (qPCR) reactions were then performed on a Bio-Rad CFX96 thermal cycler (Bio-Rad Hungary, Budapest, Hungary) using the SensiFast SYBR Green PCR Master Mix (Thermo Fisher). The specificity and efficiency of each PCR reaction was confirmed with melting curve and standard curve analysis, respectively. Each sample was quantified in duplicate and normalized to the same sample's 18S rRNA (RN18S) expression. Mean expression values were calculated as fold expression relative to a baseline control sample using the $2^{-\Delta\Delta Ct}$ formula which transforms Ct values into a biologically meaningful fold-change. If fold-change is >1, mRNA is accumulated or the cytokine gene is upregulated, and if it is < 1, there is no net mRNA uptake, or the gene is downregulated. Primer sequences for vaccine-encoded SP mRNA (expression vector BNT162b2), CCL2, CXCL10 (IP-10), IL1RA, RN18S and TNF-α are shown in Supplementary Table 1.

5.7. Histopathologic examination of pig tissues

Gross postmortem examination was made at dorsal recumbency, directly after euthanasia: after external examination, skin sample taking and skinning of the animal, we opened the body cavities and took approximately 1 cm^3 sample of organs (spleen, liver, kidneys, lymph node close to injection site, heart [from both ventricles], brain [both from cerebrum and cerebellum]) for histopathology. Histopathologic specimens were fixed in 10% neutral-buffered formalin for 24 hours at room temperature. Formalin-fixed and paraffin-embedded sections were stained with haematoxylin and eosin and submitted to routine histological examination. After the staining, slides were scanned and representative images were taken (Pannoramic Midi II slide scanner; SlideViewer software; 3DHistech, Budapest, Hungary).

5.8. Immunostaining of pig tissues

Formalin-fixed paraffin embedded kidney, heart and brain tissues were cut and 4 µm slices mounted on SuperFrost Plus slides (Thermo, USA). Heat-induced antigen retrieval was performed with citric buffer pH 6.0 for 20 minutes, then slides were blocked with 5% donkey serum for 30 minutes and stained for SP1 protein (1:400 rabbit monoclonal anti-SP1, Thermo, USA) at 4C overnight. For kidney and heart samples, the secondary antibody (1:200 biotinylated donkey anti-rabbit antibody, Jackson Immunoresearch, USA) was applied for 1 hour followed by HRP-conjugated streptavidine (1:200, Genetex, USA) and developed with Vulcan Fast Red substrate (Biocare, Pacheco, CA, USA)). Immunostaining was evaluated under Leica DM-R light microscope at 200x magnification. Brain sections were incubated with fluorescent secondary antibody (1:200, goat anti-rabbit-Alexa-594, Jackson Immunoresearch, West Grove, PA, USA) for 2 h in the dark. The slides were then covered with coverslips on VectaShield mounting medium containing DAPI (4′,6-diamidino-2-phenylindole) for nuclear staining (Vector Laboratories, Newark, CA, USA) and analyzed under a fluorescent microscope at 400x magnification.

5.9. Statistical Analyses

Data are presented as mean ± SD or mean ± SEM (in vivo data). Statistical comparisons were done with GraphPad Prism 8 (GraphPad Software Inc., San Diego, CA, USA). Cardiopulmonary parameters were evaluated using one or two-way ANOVA and Sidak's or Tukey's multiple comparisons test. Anti-PEG antibodies were analyzed by paired *t*-test. PBMC and tissue gene expression values were evaluated using Wilcoxon test. Level of significance was set to $p < 0.05$ in each analysis.

CRediT authorship contribution statement

Conceptualization, JSz, GK, LD, methodology and formal analysis GK, GSz, LD; writing/editing: JSz, GK, GSz, LD; investigation: LD, GK, CsR, TM, RF, ASz, TB, GTK, ABD; project administration and funding, JSz, TR, LD and MB. All authors have read and agreed to the published version of the manuscript.

Funding: This research was funded by the European Union Horizon 2020 projects 825828 (Expert) and 2022-1.2.5-TÉT-IPARI-KR-2022-00009, and Semmelweis University Grant STIA-KFI-2022/002 to LD. GK was also supported by the Bolyai Scholarship of the Hungarian Academy of Sciences (BO/00304/20/5) and ÚNKP Bolyai+ Scholarship from the Hungarian Ministry of Innovation and Technology and National Research, Development, and Innovation Office (ÚNKP-22-5/202206201434KG). TKP2021-EGA-23 has been implemented with the support provided by the Ministry of Innovation and Technology of Hungary from the National Research, Development and Innovation Fund. Project no. RRF-2.3.1-21-2022-00003 has been implemented with the support provided by the European Union. B.A.B. was supported by the EKÖP-2024-12 New National Excellence Program.

Institutional Review Board Statement: The study was conducted in accordance with the Declaration of Helsinki, and the animal study protocol was approved by the Institutional and National Review Board/Ethics Committees, PE/EA/843-7/2020.

Data Availability Statement: Experimental data are available upon reasonable request to the corresponding author.

Acknowledgments: The expert technical support by Dóra Szkrajcsics, Maria H. Velkei, Bojána Sipiczki, Katalin Simay, Henriett Biró and Krisztina Fazekas are gratefully acknowledged.

References

Anis, E., Preis, S. A., Cedar, N., Tal, Y., Hershkowitz, I., & Hershko, A. Y. (2022). Reporting of Allergic Reactions During Pfizer-BioNTech BNTT162B2 Vaccination in Israel. *J Allergy Clin Immunol Pract, 10*(11), 2969-2976. doi:10.1016/j.jaip.2022.07.012

Bakos, T., Meszaros, T., Kozma, G. T., Berenyi, P., Facsko, R., Farkas, H., … Szebeni, J. (2024). mRNA-LNP COVID-19 Vaccine Lipids Induce Complement Activation and Production of Proinflammatory Cytokines: Mechanisms, Effects of Complement Inhibitors, and Relevance to Adverse Reactions. *Int J Mol Sci, 25*(7) doi:10.3390/ijms25073595

Barta, B. A., Radovits, T., Dobos, A. B., Kozma, G. T., Mészáros, T., Berényi, P., … Szebeni, J. (2024). Comirnaty-induced cardiopulmonary distress and other symptoms of

complement-mediated pseudo-anaphylaxis in a hyperimmune pig model: Causal role of anti-PEG antibodies. *Vaccine: X, 19*, 100497.

Bhattacharjee, B., Lu, P., Monteiro, V. S., Tabachnikova, A., Wang, K., Hooper, W. B., … Iwasaki, A. (2025). Immunological and Antigenic Signatures Associated with Chronic Illnesses after COVID-19 Vaccination. *medRxiv, doi: https://doi.org/10.1101/2025.02.18.25322379; February 25, 2025*.

Blumenthal, K. G., Robinson, L. B., Camargo, C. A., Jr., Shenoy, E. S., Banerji, A., Landman, A. B., & Wickner, P. (2021). Acute Allergic Reactions to mRNA COVID-19 Vaccines. *JAMA, 325*(15), 1562-1565. doi:10.1001/jama.2021.3976

Boros, L. G., Kyriakopoulos, A. M., Brogna, C., Piscopo, M., McCullough, P. A., & Seneff, S. (2024). Long-lasting, biochemically modified mRNA, and its frameshifted recombinant spike proteins in human tissues and circulation after COVID-19 vaccination. *Pharmacol Res Perspect, 12*(3), e1218. doi:10.1002/prp2.1218

Bozkurt, B., Kamat, I., & Hotez, P. J. (2021). Myocarditis With COVID-19 mRNA Vaccines. *Circulation, 144*(6), 471-484. doi:10.1161/CIRCULATIONAHA.121.056135

Brogna, C., Cristoni, S., Marino, G., Montano, L., Viduto, V., Fabrowski, M., … Piscopo, M. (2023). Detection of recombinant Spike protein in the blood of individuals vaccinated against SARS-CoV-2: Possible molecular mechanisms. *Proteomics Clin Appl, 17*(6), e2300048. doi:10.1002/prca.202300048

Cheng, M. H. Y., Leung, J., Zhang, Y., Strong, C., Basha, G., Momeni, A., … Cullis, P. R. (2023). Induction of Bleb Structures in Lipid Nanoparticle Formulations of mRNA Leads to Improved Transfection Potency. *Adv Mater, 35*(31), e2303370. doi:10.1002/adma.202303370

Christopher, M. M., & Brounts, S. H. (2010). Hematologic Characteristics of Swine. (Eds.), ., pp). Wiley-Blackwell. In I. D. J. W. K. J. Wardrop (Ed.), *Schalm's Veterinary Hematology (6th ed)*, (pp. 819–824): Wiley-Blackwell.

Cullis, P. R., & Felgner, P. L. (2024). The 60-year evolution of lipid nanoparticles for nucleic acid delivery. *Nat Rev Drug Discov*doi:10.1038/s41573-024-00977-6

Dezsi, L., Meszaros, T., Kozma, G., M, H. V., Olah, C. Z., Szabo, M., … Szebeni, J. (2022). A naturally hypersensitive porcine model may help understand the mechanism of COVID-19 mRNA vaccine-induced rare (pseudo) allergic reactions: complement activation as a possible contributing factor. *Geroscience, 44*(2), 597-618. doi:10.1007/s11357-021-00495-y

Francia, V., Schiffelers, R. M., Cullis, P. R., & Witzigmann, D. (2020). The Biomolecular Corona of Lipid Nanoparticles for Gene Therapy. *Bioconjug Chem, 31*(9), 2046-2059. doi:10.1021/acs.bioconjchem.0c00366

Guo, R. F., & Ward, P. A. (2005). Role of C5a in inflammatory responses. *Annu Rev Immunol, 23*, 821-852. doi:10.1146/annurev.immunol.23.021704.115835

Jaffer, U., Wade, R. G., & Gourlay, T. (2010). Cytokines in the systemic inflammatory response syndrome: a review. *HSR Proc Intensive Care Cardiovasc Anesth, 2*(3), 161-175. Retrieved from https://www.ncbi.nlm.nih.gov/pubmed/23441054

Kany, S., Vollrath, J. T., & Relja, B. (2019). Cytokines in Inflammatory Disease. *Int J Mol Sci, 20*(23)doi:10.3390/ijms20236008

Kariko, K., Buckstein, M., Ni, H., & Weissman, D. (2005). Suppression of RNA recognition by Toll-like receptors: the impact of nucleoside modification and the evolutionary origin of RNA. *Immunity, 23*(2), 165-175. doi:10.1016/j.immuni.2005.06.008

Kauffman, K. J., Mir, F. F., Jhunjhunwala, S., Kaczmarek, J. C., Hurtado, J. E., Yang, J. H., Anderson, D. G. (2016). Efficacy and immunogenicity of unmodified and pseudouridine-modified mRNA delivered systemically with lipid nanoparticles in vivo. *Biomaterials, 109*, 78-87. doi:10.1016/j.biomaterials.2016.09.006

Kent, S. J., Li, S., Amarasena, T. H., Reynaldi, A., Lee, W. S., Leeming, M. G., … Ju, Y. (2024). Blood Distribution of SARS-CoV-2 Lipid Nanoparticle mRNA Vaccine in Humans. *ACS Nano, 18*(39), 27077-27089. doi:10.1021/acsnano.4c11652

Kozma, G. T., Meszaros, T., Vashegyi, I., Fulop, T., Orfi, E., Dezsi, L., … Szebeni, J. (2019). Pseudo-anaphylaxis to Polyethylene Glycol (PEG)-Coated Liposomes: Roles of Anti-PEG IgM and Complement Activation in a Porcine Model of Human Infusion Reactions. *ACS Nano, 13*(8), 9315-9324. doi:10.1021/acsnano.9b03942

Krumholz, H. M., Wu, Y., Sawano, M., Shah, R., Zhou, T., Arun, A. S., … Iwasaki, A. (2023). Post-Vaccination Syndrome: A Descriptive Analysis of Reported Symptoms and Patient Experiences After Covid-19 Immunization. *medRxiv posted November 10, 2023. doi: https://doi.org/10.1101/2023.11.09.23298266*doi:10.1101/2023.11.09.23298266

Lamprinou, M., Sachinidis, A., Stamoula, E., Vavilis, T., & Papazisis, G. (2023). COVID-19 vaccines adverse events: potential molecular mechanisms. *Immunol Res, 71*(3), 356-372. doi:10.1007/s12026-023-09357-5

Lieberman, P. (2008). Epidemiology of anaphylaxis. *Curr Opin Allergy Clin Immunol, 8*(4), 316-320. doi:10.1097/ACI.0b013e3283036a69

Lindsay, K. E., Bhosle, S. M., Zurla, C., Beyersdorf, J., Rogers, K. A., Vanover, D., … Santangelo, P. J. (2019). Visualization of early events in mRNA vaccine delivery in non-human primates via PET-CT and near-infrared imaging. *Nat Biomed Eng, 3*(5), 371-380. doi:10.1038/s41551-019-0378-3

McCullough, P. A., & Hulscher, N. (2025). Risk stratification for future cardiac arrest after COVID-19 vaccination. *World J Cardiol, 17*(2), 103909. doi:10.4330/wjc.v17.i2.103909

Ndeupen, S., Qin, Z., Jacobsen, S., Bouteau, A., Estanbouli, H., & Igyarto, B. Z. (2021). The mRNA-LNP platform's lipid nanoparticle component used in preclinical vaccine studies is highly inflammatory. *iScience, 24*(12), 103479. doi:10.1016/j.isci.2021.103479

Nurnberger, W., Michelmann, I., Eckhof-Donovan, S., Bockmann, D., Petrik, K., Gobel, G., … Gobel, U. (1994). Platelet consumption and activation of the complement system induced by infusion of rTNF alpha and rIFN gamma. *Ann N Y Acad Sci, 714*, 291-292. doi:10.1111/j.1749-6632.1994.tb12058.x

Oueijan, R. I., Hill, O. R., Ahiawodzi, P. D., Fasinu, P. S., & Thompson, D. K. (2022). Rare Heterogeneous Adverse Events Associated with mRNA-Based COVID-19 Vaccines: A Systematic Review. *Medicines (Basel), 9*(8)doi:10.3390/medicines9080043

Palmer, M., Bhakdi, S., Hooker, B., Holland, M., DesBois, M., Rasnick, D., & Fitts, C. A. (2023). *mRNA vVaccine Toxicity*. https://d4ce.org/mRNA-vaccine-toxicity/.

Pardi, N., Hogan, M. J., Porter, F. W., & Weissman, D. (2018). mRNA vaccines - a new era in vaccinology. *Nat Rev Drug Discov, 17*(4), 261-279. doi:10.1038/nrd.2017.243

Pardi, N., Tuyishime, S., Muramatsu, H., Kariko, K., Mui, B. L., Tam, Y. K., … Weissman, D. (2015). Expression kinetics of nucleoside-modified mRNA delivered in lipid nanoparticles to mice by various routes. *J Control Release, 217*, 345-351. doi:10.1016/j.jconrel.2015.08.007

Pfizer Australia (2021). Nonclinical Evaluation Report: BNT162b2 [mRNA] COVID-19 vaccine (COMIRNATYTM). *https://www.tga.gov.au/sites/default/files/foi-2389-06.pdf, https://t.co/Zrhakh7Xgv*.

Schlake, T., Thess, A., Fotin-Mleczek, M., & Kallen, K. J. (2012). Developing mRNA-vaccine technologies. *RNA Biol, 9*(11), 1319-1330. doi:10.4161/rna.22269

Schreckenberg, R., Woitasky, N., Itani, N., Czech, L., Ferdinandy, P., & Schulz, R. (2024). Cardiac side effects of RNA-based SARS-CoV-2 vaccines: Hidden cardiotoxic effects of mRNA-1273 and BNT162b2 on ventricular myocyte function and structure. *Br J Pharmacol, 181*(3), 345-361. doi:10.1111/bph.16262

Shavit, R., Maoz-Segal, R., Iancovici-Kidon, M., Offengenden, I., Haj Yahia, S., Machnes Maayan, D., … Agmon-Levin, N. (2021). Prevalence of Allergic Reactions After Pfizer-BioNTech COVID-19 Vaccination Among Adults With High Allergy Risk. *JAMA Netw Open, 4*(8), e2122255. doi:10.1001/jamanetworkopen.2021.22255

Shimabukuro, T. T., Cole, M., & Su, J. R. (2021). Reports of Anaphylaxis After Receipt of mRNA COVID-19 Vaccines in the US-December 14, 2020-January 18, 2021. *JAMA, 325*(11), 1101-1102. doi:10.1001/jama.2021.1967

Shrestha, Y., & Venkataraman, R. (2024). The prevalence of post-COVID-19 vaccination syndrome and quality of life among COVID-19-vaccinated individuals. *Vacunas, 25*(1), 7-18. doi:https://doi.org/10.1016/j.vacun.2023.10.002

Sims, P. J., & Wiedmer, T. (1991). The response of human platelets to activated components of the complement system. *Immunol Today, 12*(9), 338-342. doi:10.1016/0167-5699(91)90012-I

Sindet-Pedersen, C., Michalik, F., Strange, J. E., Christensen, D. M., Nouhravesh, N., Gerds, T. A., … Schou, M. (2023). Risk of Worsening Heart Failure and All-Cause Mortality Following COVID-19 Vaccination in Patients With Heart Failure: A Nationwide Real-World Safety Study. *Circ Heart Fail, 16*(10), e010617. doi:10.1161/CIRCHEARTFAILURE.123.010617

Szebeni, J. (2024). Evaluation of the Acute Anaphylactoid Reactogenicity of Nanoparticle-Containing Medicines and Vaccines Using the Porcine CARPA Model. In Jeffrey D. Clogston et al. (eds.) (Ed.), *Characterization of Nanoparticles Intended for Drug Delivery, ttps://doi.org/10.1007/978-1-0716-3786-9_23,* . https://doi.org/10.1007/978-1-0716-3786-9_23.

Szebeni, J. (2025a). Expanded Spectrum and Increased Incidence of Adverse Events Linked to COVID-19 Genetic Vaccines: New Concepts on Prophylactic Immuno-Gene Therapy, Iatrogenic Orphan Disease, and Platform-Inherent Challenges. *Pharmaceutics, 17*(4), 450. Retrieved from https://www.mdpi.com/1999-4923/17/4/450

Szebeni, J. (2025b). The Unique Features and Collateral Immune Effects of mRNA-Based COVID-19 Vaccines: Potential Plausible Causes of Adverse Events and Complications. In *Preprints*: Preprints.

Szebeni, J., Bedocs, P., Urbanics, R., Bunger, R., Rosivall, L., Toth, M., & Barenholz, Y. (2012). Prevention of infusion reactions to PEGylated liposomal doxorubicin via tachyphylaxis induction by placebo vesicles: a porcine model. *J Control Release, 160*(2), 382-387. doi:10.1016/j.jconrel.2012.02.029

Turner, P. J., Jerschow, E., Umasunthar, T., Lin, R., Campbell, D. E., & Boyle, R. J. (2017). Fatal Anaphylaxis: Mortality Rate and Risk Factors. *J Allergy Clin Immunol Pract, 5*(5), 1169-1178. doi:10.1016/j.jaip.2017.06.031

Warren, C. M., Snow, T. T., Lee, A. S., Shah, M. M., Heider, A., Blomkalns, A., … Nadeau, K. C. (2021). Assessment of Allergic and Anaphylactic Reactions to mRNA COVID-19 Vaccines With Confirmatory Testing in a US Regional Health System. *JAMA Netw Open, 4*(9), e2125524. doi:10.1001/jamanetworkopen.2021.25524

Wei, L., Dong, C., Zhu, W., & Wang, B. Z. (2024). mRNA Vaccine Nanoplatforms and Innate Immunity. *Viruses, 16*(1) doi:10.3390/v16010120

Zelkoski, A. E., Lu, Z., Sukumar, G., Dalgard, C., Said, H., Alameh, M. G., … Malloy, A. M. W. (2025). Ionizable lipid nanoparticles of mRNA vaccines elicit NF-kappaB and IRF responses through toll-like receptor 4. *NPJ Vaccines, 10*(1), 73. doi:10.1038/s41541-025-01124-x

SUPPLEMENTARY information

STable 1. Primer sequences for qPCR analysis

Gene Symbol	Forward Primer	Reverse Primer
SP (OR134577)	AAGAGATTCGACAACCCCGT	GCACACTTTGATGACCACGT
***ssCCL2* (NM_214214)**	GAAGCAGTGATCTTCAAGAC	GGGCAAGTTAGAAGGAAATG
***ssCXCL10* (NM_001008691)**	TGCAGCACCATGAACCAAAG	CTGGAGAGAGGTATTCCTTGAGT
***ssIL1RA* (NM_214262)**	CAAGCCTTCAGAATCTGGGATGTC GGCTCAACAGGCACCACATC	GGCTCAACAGGCACCACATC
***ssRN18S* (NR_046261)**	GACAAATCGCTCCACCAACT	CCTGCGGCTTAATTTGACTC
***ssTNFa* (NM_214022)**	GGCCCAAGGACTCAGATCAT	CTGTCCCTCGGCTTTGACAT

STable 2. Histopathological evaluation of organ specimens obtained from pigs 6h post-treatment

Tissue type	**Skin**	**Brain**	**Cardiac muscle**	**Lymph node**	**Spleen**	**Liver**	**Kidney**
Code							
#16	no lesions	no lesions	no lesions	well recognizable follicular structure	well recognizable follicular structure, passive hyperemia due to anesthesia	physiological prominent interlobular connective tissue septae, normal histological structure, intact portal tracts, mild intracytoplasmic vacuolisation diffusely	intact glomerular and tubular structure

#1	no lesions	NA	no lesions	mild lymphopenia	no lesions	mild sinusoidal and perivascular hyperemia (v. centralis)	no lesions
#2	NA	NA	no lesions	no lesions	no lesions	no lesions	no lesions
#3	no lesions	mild neuropil vacuolisation	no lesions	NA	no lesions	multifocal hemorrhages and single cell to massive necrosis; focal, mild neutrophilic and lymphocytic periportal infiltration; moderate intracytoplasmic vacuolisation diffusely	mild basilar intracytoplasmic vacuolisation in the tubular epithelial cells
#4	NA	mild neuropil vacuolisation	no lesions	no lesions	no lesions	no lesions	multifocal tubular dilation with flattened tubular epithelial cells
#5	no lesions	mild neuropil vacuolisation	no lesions	mild lymphopenia	no lesions	no lesions	multifocal prominent tubular dilation with normal cuboidal tubular epithelial cells

#8	no lesions	mild vascular edema; mild neuropil vacuolisation	no lesions	no lesions	no lesions	no lesions	no lesions
#9	no lesions	mild vascular edema; mild neuropil vacuolisation	NA	NA	no lesions	mild sinusoidal and perivascular hyperemia (v. centralis)	multifocal tubular dilation with flattened tubular epithelial cells

Pig with code #16 is a control animal with physiological histology of organs (SPF animal). NA: not applicable/no organs were submitted to evaluation. STable 2 shows mild neuropil vacuolisation of the brain specimens in almost all cases, and mild vascular edema in #8 and #9 – this can correlate with hypoxia-induced edema. Still, it can also appear artifactually due to processing. However, we could not detect neuropil vacuolisation, nor vascular edema in the control animal's brain tissue, therefore, the possibility of being only an artefact is low. Skin samples were taken from the administration sites. Still, no pathologic lesions were detected. Although there was mild reactivity with immunostaining of SP in myocardium, we observed no histopathologic effects on the cardiac muscle tissues. In the spleen and regional lymph node tissues, we observed mild lymphopenia in two cases, which probably does not correlate with the vaccine administration. During the examination of liver specimens, some showed mild perivascular and/or sinusoidal hyperemia, which can occur during anaesthesia; however, in pig #3 we detected mild to moderate necrotizing hepatitis. As it was a single case, the relation of cause and effect between vaccination and the hepatic pathology is highly questionable; it is more likely that this pig had a viral/bacterial infection – further examination would be needed to rule this out. We observed a few tubular cysts in the kidney sections, with either flattened or normal cuboidal epithelial cells, or mild hyperemia. Cyst formation in the swine renal cortex is often an accidental finding. In conclusion, we can say that no major pathologies were detected in these specimens, except pig #3.

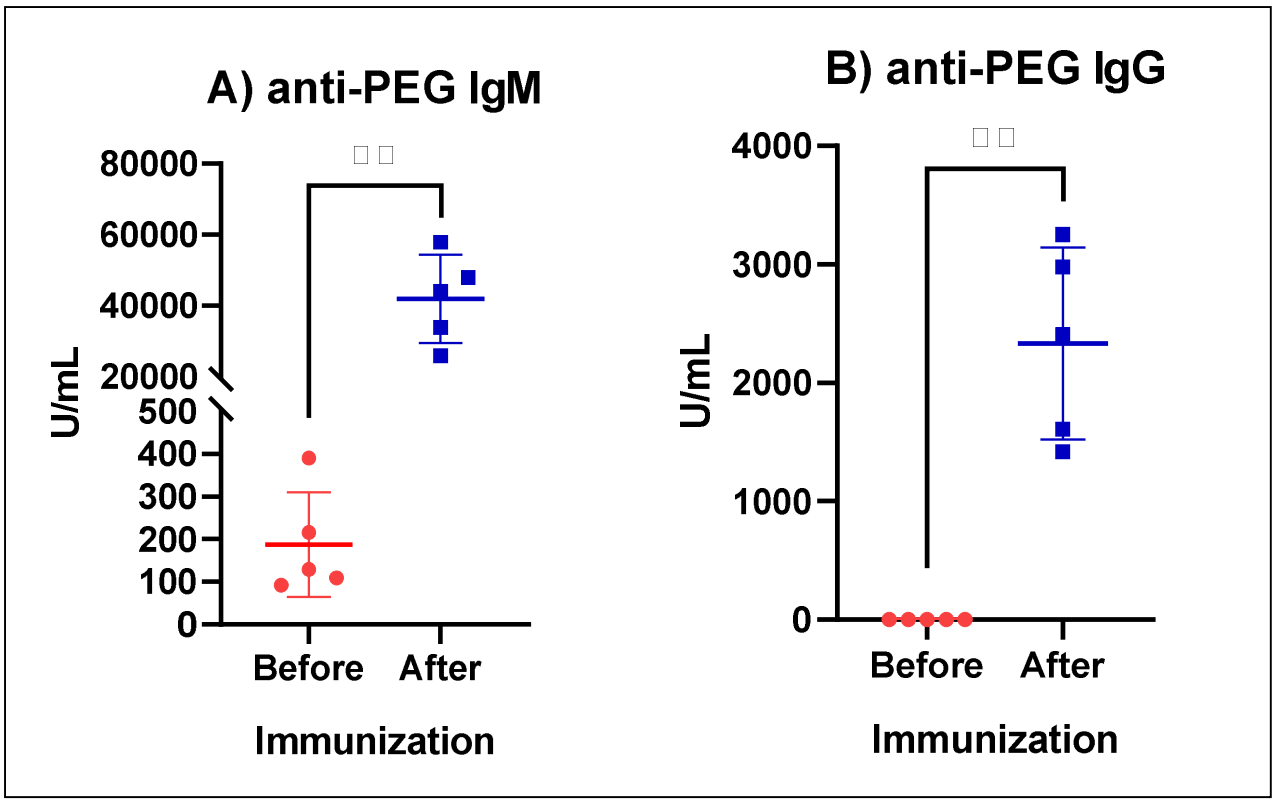

SFigure 1 The induction of anti-PEG IgM and IgG by PEGylated doxorubicin-free liposomes. A) anti-PEG IgM and B) anti-PEG IgG one week after i.v. infusion of pigs with Doxebo. Values are mean ± SD, n= 5 pigs

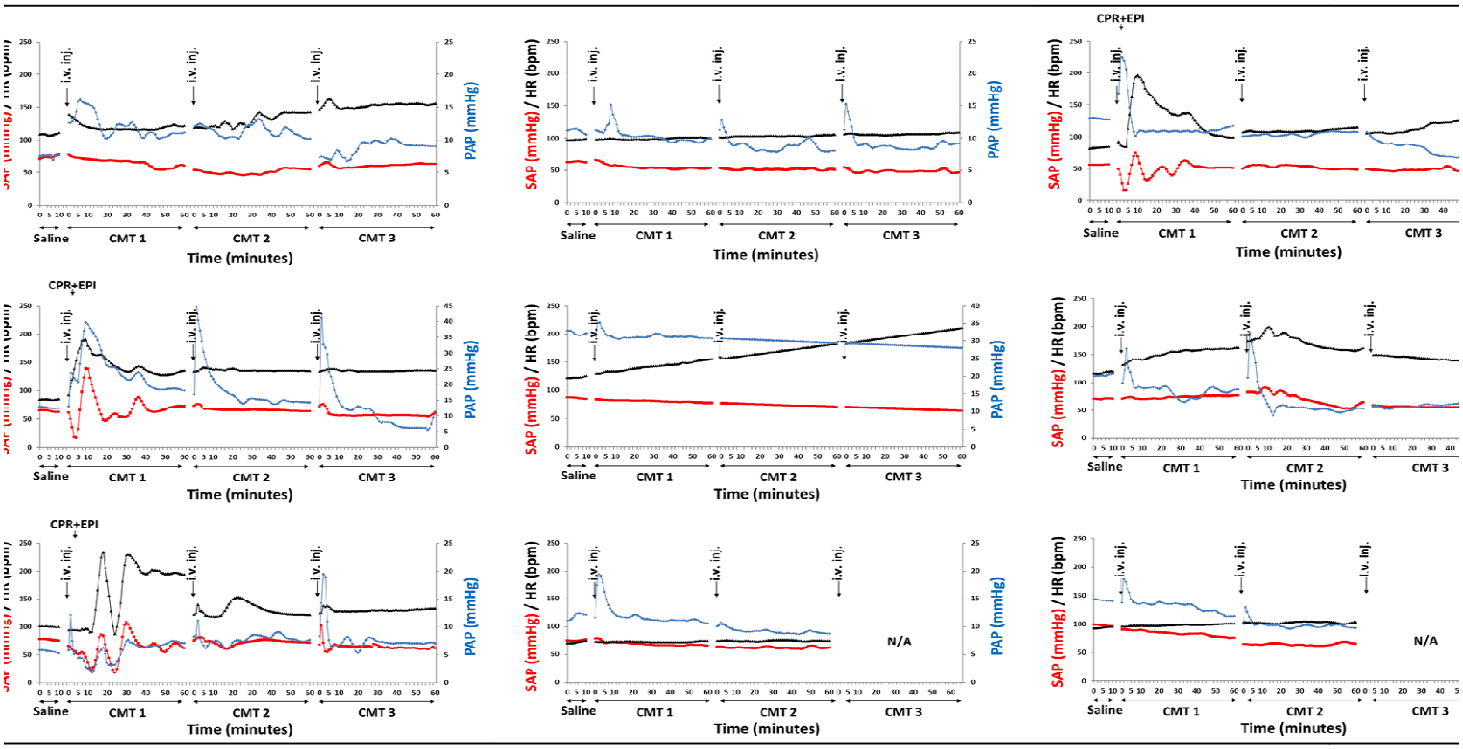

SFigure. 2 Cardiovascular changes in individual pigs following acute i.v. vaccination with 3x HVD of Comirnaty vaccine**.** CMT – Comirnaty vaccine, SAP –Systemic Arterial Pressure, HR – Heart Rate, PAP – Pulmonary Arterial Pressure. CPR – Cardio-Pulmonary Resuscitation, EPI - Epinephrine